Letter

Engineering Casimir interactions with epsilon-near-zero materials

Miguel Camacho ,[1,2] Tao Gong ,[3,4] Benjamin Spreng ,[3] Iñigo Liberal,[5] Nader Engheta ,[1,*] and Jeremy N. Munday [3,†]

[1]*Department of Electrical and Systems Engineering, University of Pennsylvania, Philadelphia, Pennsylvania 19104, USA*
[2]*Department of Electronics and Electromagnetism, Universidad de Sevilla, 41012 Seville, Spain*
[3]*Department of Electrical and Computer Engineering, University of California, Davis, California 95616, USA*
[4]*Department of Materials Science and Engineering, University of California, Davis, California 95616, USA*
[5]*Department of Electrical and Electronic Engineering, Public University of Navarra, 31006 Pamplona, Spain*

(Received 10 December 2021; accepted 10 May 2022; published 3 June 2022)

In this paper, we theoretically demonstrate the tunability of the Casimir force both in sign and magnitude between parallel plates coated with dispersive materials. We show that this force, existing between uncharged plates, can be tuned by carefully choosing the value of the plasma frequency (i.e., the epsilon-near-zero frequency) of the coating in the neighborhood of the resonance frequency of the cavity. The coating layer enables a continuous variation of the force between four limiting values when a coating is placed on each plate. We explore the consequences of such variation when pairs of electric and magnetic conductors (i.e., low and high impedance surfaces) are used as substrates on either side, showing that this continuous variation results in changes in the sign of the force, leading to both stable and unstable conditions, which could find interesting potential applications in nanomechanics, including nanoparticle tweezing.

DOI: 10.1103/PhysRevA.105.L061501

I. INTRODUCTION

The surprising existence of a force between two parallel metal plates in the absence of electric charges was predicted by Casimir in 1948 by means of an estimation of the rate of change of the zero-point energy associated with quantum electrodynamic fluctuations [1].

It was Lifshitz who several years later presented an exhaustive mathematical formulation for the calculation of such a force, which was already understood as being responsible for the attractive force between neutral molecular structures [2]. Due to the continuous frequency spectrum of the quantum fluctuations, the resulting force is given by a slowly convergent integral over all frequencies, for which Lifshitz presented an expression in the form of an integral over imaginary frequencies with rapid convergence associated with the exponential decay of quantum electrodynamic fluctuations [3–5].

Due to the small amplitude of these forces, their experimental validation remained elusive for many years [6], and it was not until recently that their role in nanostructures with more complex interactions was explored [7–9].

The ability to engineer its wideband frequency and wavevector net contributions launched the quest for materials that would allow for the manipulation of both the magnitude and sign of the total net Casimir force [10,11], including the use of complex artificial materials known as metamaterials [12] and different combinations of boundary conditions such as mirrors including electric, magnetic, and electromagnetic conductors [13–15]. In [16], it was shown that one can achieve repulsive Casimir forces for a wide distance range with naturally occurring materials. More recently, the combination of attractive and repulsive Casimir forces was achieved using multilayered stacks to allow for stable trapping conditions in fluids, which could find applications in nanomechanics [17,18]. It was also demonstrated that anisotropic materials can lead to Casimir torques [19].

Most studies considered metallic materials acting as good conducting mirrors. Therefore, in such scenarios, the plasma frequency, corresponding to the frequency point where the real part of the permittivity crossed zero, occurred at frequencies that contributed little to the net Casimir interaction. However, the field of epsilon-near-zero (ENZ) optics, i.e., materials and photonic structures with near-zero permittivity, has attracted a lot of attention due to its unusual wave effects [20]. For example, these materials allow for special types of resonances that are able to selectively annihilate quantum fluctuations, which are, in turn, responsible for the Casimir force [21].

In this paper, we theoretically demonstrate the possibilities offered by low-plasma-frequency materials for tailoring the Casimir force between high and low impedance surfaces (i.e., highly conducting or impeding surfaces). Specifically, we show that it is possible to achieve attractive and repulsive interactions with both stable and unstable equilibria that can be controlled by tailoring the plasma frequency, layer thickness, and/or surface separation.

II. COATED ELECTRIC CONDUCTORS

Let us consider two parallel perfect electric conductor (PEC) surfaces, each coated with a slab whose permittivities

*engheta@ee.upenn.edu
†jnmunday@ucdavis.edu

follow the Drude dispersion model given by

$$\varepsilon_i(\omega) = 1 - \frac{\omega_{pi}^2}{\omega(\omega - i\omega_{ci})}, \tag{1}$$

with plasma frequencies ω_{p1} and ω_{p2} for the left and right coatings, respectively, and negligible losses ($\omega_{c1} = \omega_{c2} \approx 0$) for an assumed harmonic time dependence $e^{i\omega t}$. Although low loss has been assumed for simplicity here, small losses ($\omega_c < \omega_p/10$) have been found to have negligible effects on the results presented here, which are consistent with measured values for ENZ materials such as ITO [22]. Nevertheless, the inclusion of losses in the Lifshitz formula were shown in some cases to lead to inaccurate results when compared to experiments; as such the effects of large losses remain an open question [7,23].

As presented by Liftshitz, the Casimir pressure can be calculated in terms of an integral over the imaginary frequency $\xi = i\omega$ and real wave vector p, obtained through a rotation of the integration paths both in frequency and wave vector, given by [4]

$$P = -\frac{\hbar}{2\pi^2 c^3}\int_0^\infty d\xi \int_1^\infty dp\, \xi^3 p^2 \times \left[\frac{\Delta_L\,\Delta_R e^{-r_n p}}{1 - \Delta_L\,\Delta_R e^{-r_n p}} + \frac{\overline{\Delta_L}\,\overline{\Delta_R} e^{-r_n p}}{1 - \overline{\Delta_L}\,\overline{\Delta_R} e^{-r_n p}}\right], \tag{2}$$

where Δ_L and $\overline{\Delta_L}$ correspond to the reflection coefficients at the interface between a vacuum and the multilayered medium on the left for transverse electric and transverse magnetic polarizations, respectively, and similarly for Δ_R and $\overline{\Delta_R}$ with respect to the right side of the cavity and $r_n = 2\ell\xi/c$ with c representing the speed of light in a vacuum, where ℓ is the vacuum-filled distance between the two surfaces. In particular, for singly coated media on the left side, one can calculate the multilayer effective reflection coefficients for the transverse electric polarization using the expression [4,24,25]

$$\Delta_L = \frac{\Delta_{LA_1} e^{-2s_{A_1} d_1} + \Delta_{A_1 m}}{1 + \Delta_{LA_1}\Delta_{A_1 m} e^{-2s_{A_1} d_1}}, \tag{3}$$

where Δ_{LA_1} is the reflection coefficient between the coating material and the semi-infinite medium on the left side, $\Delta_{A_1 m}$ is the reflection coefficient between the vacuum and the coating material, s_{A_1} is the wave vector in the coating material given in terms of p by

$$s_{A_1} = \sqrt{p^2 - 1 + \varepsilon_{rA_1}\mu_{rA_1}}, \tag{4}$$

and likewise for the transverse magnetic polarization, $\overline{\Delta_L}$ using the appropriate $\overline{\Delta_{LA_1}}$ and $\overline{\Delta_{A_1 m}}$ reflection coefficients.

The reflection coefficients between media A and B for the two polarizations can be calculated using

$$\Delta_{AB} = \frac{s_B\mu_A - s_A\mu_B}{s_B\mu_A + s_A\mu_B}, \tag{5}$$

$$\overline{\Delta_{AB}} = \frac{s_B\varepsilon_A - s_A\varepsilon_A}{s_B\varepsilon_A + s_A\varepsilon_B}. \tag{6}$$

In the presence of more layers, an iterative procedure can be followed to obtain the global reflection coefficients as shown in [4,24].

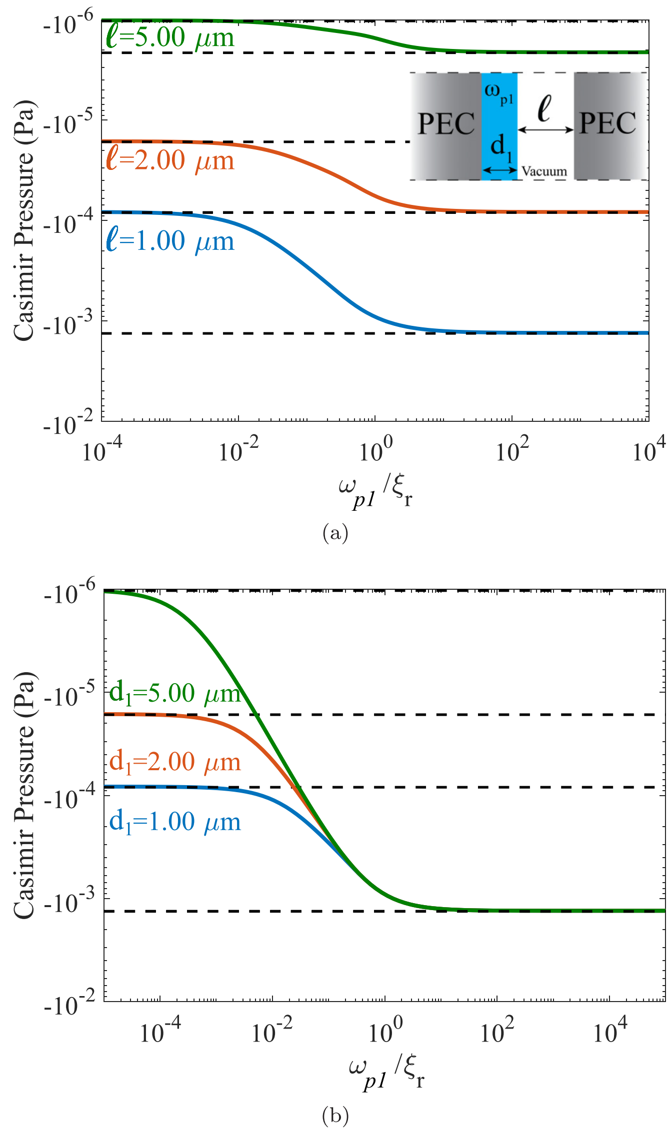

FIG. 1. Casimir pressure dependence on the plasma frequency (relative to the expected lowest resonance of the cavity formed by two highly conductive walls ξ_r) for a cavity coated only on one side ($d_1 = 1\,\mu$m and $d_2 = 0$) for (a) three different distances ℓ and (b) three different coating thicknesses d_1 with $\ell = 1\,\mu$m.

From Eq. (2), one can obtain a simple expression for the force in the absence of dielectric coatings when the two mirrors are assumed to be perfect electric conductors and at zero temperature, given by [1,26]

$$P_E = -\frac{\pi^2\hbar c}{240\ell^4}, \tag{7}$$

where the negative sign of the pressure corresponds to attraction, while a positive sign corresponds to repulsion.

As the starting point, we study the effect of changing the plasma frequency of one of the two coating layers, with constant thickness $d_1 = 1\,\mu$m in the absence of the second coating, i.e., $d_2 = 0$. We present these results in Fig. 1(a), where one finds that, as the plasma frequency is modified, the net attractive Casimir pressure (i.e., force per unit surface) is swept between two limiting values. These two limiting values correspond to the coating layer acting either as a vacuum or as a perfectly conducting material for low and high values of the plasma frequency, respectively (given by the black dashed lines). This can be explained by the fact that the integral in Eq. (2) is dominated by the behavior of the materials involved around the imaginary frequency associated with the size of the cavity $\xi_r = 2\pi c/\ell$. We show that this rationale holds for three different separations between the uncoated and coated plates. For the same reason, the maximal variation of the Casimir pressure takes place when choosing a plasma frequency near to that associated with the cavity size. In this manner, one can design the amplitude of the attractive Casimir interaction by tuning the plasma frequency of the coating layer. To model the PEC surfaces, they were substituted by semi-infinite media with very low impedances, achieved by imposing a very low magnetic permeability and very high dielectric permittivity [27].

In Fig. 1(b) we complement the analysis by considering the case of constant separation between the interfaces on either side of the vacuum region (kept as $\ell = 1\ \mu$m) while we modify the thickness of the Drude-dispersive coating. We find that, in this case, as expected by our rationale, the limiting value of the pressure associated with the highly conductive regime of the coating is kept as a constant for the three cases studied. On the other hand, the second limiting value (associated with a vacuum-filled gap) is varied as the distance between the backing mirrors is increased consequently. In this case, we find that as the two limiting values become more distant, the transition region is increased and it provides the opportunity to tune in more detail the total pressure achieved using this multilayer system. It can also be concluded from the figure that the pressure exhibits a monotonically increasing behavior with respect to the plasma frequency.

Let us now consider the effect of including a coating layer on both sides, for instance, by choosing $d_1 = \ell = 1\ \mu$m and $d_2 = 2\ \mu$m. In this case, we can tune the plasma frequencies of the two coating layers, finding a more complex interaction. However, using the rationale presented before, we can expect to achieve four limiting values for the pressure, dictated by the combination of effective separations when considering none, either, or both coating materials as a highly conductive (i.e., low-impeding) material. As shown by the results in Fig. 2, by considering the possible combinations of plasma frequencies, we achieve all possible values in between these expected values of the pressure, which are in all cases attractive.

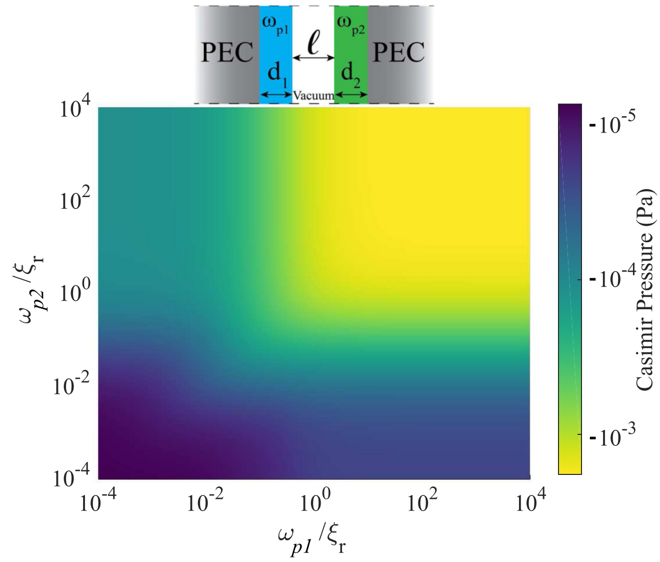

FIG. 2. Pressure dependence on the two plasma frequencies (relative to the expected lowest resonance of the cavity formed by two highly conductive walls ξ_r) for a cavity coated on both sides ($d_1 = \ell = 1\ \mu$m and $d_2 = 2\ \mu$m) for a constant separation $\ell = 1\ \mu$m.

III. COATED LOW AND HIGH IMPEDANCE SURFACES

With the understanding developed in the previous section for pairs of highly conductive plates coated with dispersive layers, let us now consider the use of high impedance surfaces, which act as perfect magnetic conductor (PMC) boundary conditions, imposing a zero tangential component of the magnetic field. These allow to modify the reflection coefficients involved in the calculation of the Casimir pressure in Eq. (2), which was shown in the literature to lead to attractive or repulsive Casimir pressures when different boundary conditions are combined [28]. For instance, both PEC-PEC (low-low impedance) and PMC-PMC (high-high impedance) cavities lead to attractive pressures, while a PEC-PMC (low-high impedance) cavity gives rise to a repulsive pressure. By adding an epsilon-near-zero coating into a PEC-PMC coating, we aim to manipulate both attractive and repulsive pressure components such that they can be balanced in a stable fashion.

Similarly to Fig. 1, in Fig. 3 we consider the problem of a cavity formed by a high impedance wall on the left side and a zero impedance wall on the right side, only the first wall being coated with a Drude-dispersive dielectric. For our analysis here, we assume the PMC to be nondispersive. Using the physical picture presented earlier, one would expect that in the high-plasma frequency regime it would behave as a cavity formed by two highly conductive walls, therefore leading to an attractive Casimir pressure. However, in contrast to the previous section, now as the dielectric coating becomes more transparent, the waves encounter a high impedance material, which leads to a repulsive pressure. To achieve the high impedance material, we can use a semi-infinite medium with very small dielectric permittivity and very high magnetic permeability [27].

Figure 3(a) shows the Casimir pressure map for a range of distances and values of the plasma frequencies. There we find the predicted crossing of the pressure through a zero value at a distance, which is a function of the chosen plasma frequency. For a fixed distance, on either side of such crossing in terms of plasma frequency, we find two pressures of different signs whose magnitudes asymptotically approach those associated with either the smaller and larger cavities formed by the interfaces. Surprisingly, if one fixes the plasma frequency and varies the distance, it is apparent that there are two equilibrium points (one stable and one unstable) for a wide range of plasma frequencies up to 90 THz, whose distance grows rapidly as the plasma frequency decreases.

As we show in Fig. 3(c) by normalizing the plasma frequency to $\xi_r = 2\pi c/\ell$ in each case, the zero-pressure crossing

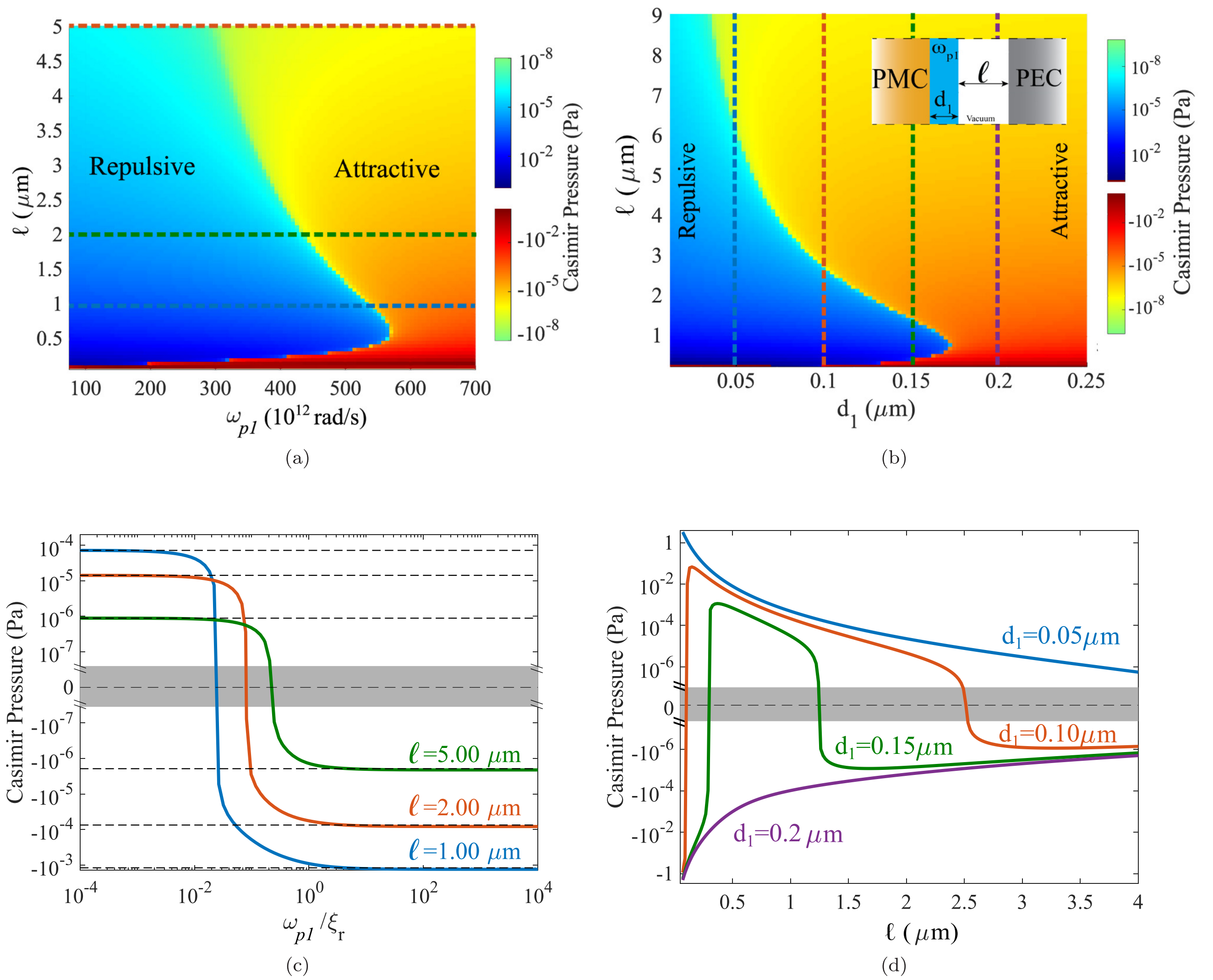

FIG. 3. Pressure dependence on the plasma frequency of the coating and separation for a cavity formed by a highly conductive wall and a coated nondispersive high impedance ($d_1 = 0.15\,\mu$m and $d_2 = 0$). Positive (negative) sign is associated with a repulsive (attractive) pressure. Panel (a) shows the pressure dependence on both the cavity separation and plasma frequency of the coating for $d_1 = 0.15\,\mu$m and panel (b) shows the pressure dependence on both the cavity separation and coating thickness for a plasma frequency of 80 THz. Panel (c) represents the extracted curves of the cuts shown in (a) and similarly between panels (d) and (b).

appears at plasma frequencies close but below that associated with the size of the cavity. Additionally, such crossings occur within a small range of relative plasma frequency and could lead to highly sensitive sensors for small displacements and material property variations. For example, with $\ell = 1\,\mu$m, half an order of magnitude change in ω_{p1}/ξ_r results in a five orders of magnitude pressure change and with an order of magnitude change one achieves the switch from attraction to repulsion. Also in Fig. 3(c) we show the asymptotic predictions for the limits of PEC coating on either side (i.e., $\omega_p \to \infty$) using Eq. (7) and for the limit of the PEC/PMC cavity, given by $P_R = -(7/8)P_E$ [28–30]. Further information on how these change at finite temperature can be found elsewhere [31,32].

To shed light on the parametric dependencies of the stability and instability points associated with the zero Casimir pressure, in Fig. 3(b) we present the pressure dependence on the thicknesses of the vacuum and dispersive regions within the cavity formed by a perfect electric and coated nondispersive magnetic conductors. For that we chose a plasma frequency of 80 THz. In there, we find that the distance at which the pressure nulls does not vary monotonically with the thickness of the dispersive layer, which is a remarkable phenomenon. In fact, this effect allows us to find equilibrium points with both stability and instability conditions at different distances. For instance, we find a coating layer with a thickness d_1 of $0.15\,\mu$m would present an unstable equilibrium point at $\ell \approx 0.3\,\mu$m and a stable equilibrium point at $\ell \approx 1.2\,\mu$m. As the thickness of the dispersive coating is reduced, the two equilibrium points become more distant. This effect is better depicted in Fig. 3(d), where the Casimir pressure is shown for a range of distances for four different coating thicknesses. In some cases (for instance, when d_1 is smaller than $0.1\,\mu$m), we find that one of the equilibrium points (the unstable one) is at a distance which is too close to be practically accessible. However, one way to exchange the stability of these zero-pressure points would be to remove the dispersive coating of the PMC and coat the PEC mirror with a permeability-dispersive layer instead.

The previous results were obtained for an arbitrary choice of the plasma frequency at 80 THz. To demonstrate that the existence of stability and instability points is independent of that choice, we performed further simulations considering a realistic ENZ material: indium tin oxide (ITO) [33].

For the case of ITO, the plasma frequency rests around 243 THz [34], leading to a pressure map similar to that in Fig. 3(b) centered around a 0.2-micron separation with the single zero-force point appearing around 0.055-micron thickness. For instance, an ITO coating layer of 0.05 microns would lead to a stable point around 0.4-micron distance and an unstable point at 0.1-micron distance. From these results, we also studied the force that a perfect electrically conducting sphere of 100-micron radius would experience over an ITO-coated perfect magnetic conductor, which leads to the same stable and unstable conditions with a force magnitude on the order of pico-Newtons.

Additionally, the high impedance wall (i.e., the PMC) could be achieved in practice using high permeability materials such as yttrium iron garnet, which has shown a strong potential for repulsive Casimir forces at room temperature [35]. The finite temperature leads to a discretization of the integral in Eq. (2), with the first term (zero frequency, at which the impedance is high) being dominant [36].

IV. CONCLUSION

In this paper, we theoretically address the problem of the Casimir pressure between impedance boundaries (high and low impedances) with the addition of dielectric layers whose permittivity is frequency-dispersive in terms of a Drude model. We show that when the plasma frequency is near the wavelength associated with the distance between the plates, the Casimir pressure can be designed by properly tuning the plasma frequency. Building on that rationale, we show that, when two different boundaries are included (a cavity made of a combination of high and low impedance walls), the pressure can be tuned between repulsive and attractive, with a zero-pressure crossing in between. We find that those equilibrium points can be designed to be either unstable or stable at either close or far distances between the plates when compared to the thickness of the coating layer and their locations can be tuned by varying the plasma frequency of the coating.

ACKNOWLEDGMENTS

The authors wish to acknowledge financial support from the Defense Advanced Research Program Agency (DARPA) QUEST program Grant No. HR00112090084. The work of MC was partially funded by Grant No. PID2020-116739GB-I00 funded by MCIN/AEI/10.13039/501100011033.

[1] H. BG. Casimir, Proc. Kon. Ned. Akad. Wet. **51**, 793 (1948).
[2] E. M. Lifshitz, J. Exp. Theor. Phys. **2**, 73 (1956).
[3] L. H. Ford, Phys. Rev. A **48**, 2962 (1993).
[4] V. A. Parsegian, *Van der Waals Forces: A Handbook for Biologists, Chemists, Engineers, and Physicists* (Cambridge University Press, Cambridge, England, 2005).
[5] S. A. Ellingsen, Europhys. Lett. **82**, 53001 (2008).
[6] B. V. Derjaguin, Y. I. Rabinovich, and N. V. Churaev, Nature (London) **272**, 313 (1978).
[7] G. L. Klimchitskaya, U. Mohideen, and V. M. Mostepanenko, Rev. Mod. Phys. **81**, 1827 (2009).
[8] A. W. Rodriguez, F. Capasso, and S. G. Johnson, Nat. Photon. **5**, 211 (2011).
[9] T. Gong, M. R. Corrado, A. R. Mahbub, C. Shelden, and J. N. Munday, Nanophotonics **10**, 523 (2021).
[10] O. Kenneth, I. Klich, A. Mann, and M. Revzen, Phys. Rev. Lett. **89**, 033001 (2002).
[11] R. Zhao, T. Koschny, E. N. Economou, and C. M. Soukoulis, Phys. Rev. B **83**, 075108 (2011).
[12] F. S. Rosa, D. A. Dalvit, and P. W. Milonni, Phys. Rev. Lett. **100**, 183602 (2008).
[13] V. N. Markov and Y. M. Pis'mak, J. Phys. A: Math. Gen. **39**, 6525 (2006).
[14] A. Romeo and A. A. Saharian, J. Phys. A: Math. Gen. **35**, 1297 (2002).
[15] S. Rode, R. Bennett, and S. Y. Buhmann, New J. Phys. **20**, 043024 (2018).
[16] J. N. Munday, F. Capasso, and V. A. Parsegian, Nature (London) **457**, 170 (2009).
[17] X. Zhang, R. Zhao, L. Li, S. Yang, W. Bao, Y. Xia, P. Ashby, and Y. Wang, Science **364**, 984 (2019).
[18] L. Ge, X. Shi, L. Liu, and K. Gong, Phys. Rev. B **102**, 075428 (2020).
[19] D. A. Somers, J. L. Garrett, K. J. Palm, and J. N. Munday, Nature (London) **564**, 386 (2018).
[20] I. Liberal and N. Engheta, Nat. Photon. **11**, 149 (2017).
[21] I. Liberal and N. Engheta, Proc. Natl. Acad. Sci. USA **114**, 822 (2017).
[22] M. Losurdo, M. Giangregorio, P. Capezzuto, G. Bruno, R. De Rosa, F. Roca, C. Summonte, J. Plá, and R. Rizzoli, J. Vac. Sci. Technol. A **20**, 37 (2002).
[23] M. Bordag, G. Klimchitskaya, U. Mohideen, and V. M. Mostepanenko, *Advances in the Casimir Effect* (Oxford University Press, Oxford, 2009).
[24] R. Podgornik, P. L. Hansen, and V. A. Parsegian, J. Chem. Phys. **119**, 1070 (2003).
[25] R. Podgornik, R. H. French, and V. A. Parsegian, J. Chem. Phys. **124**, 044709 (2006).
[26] P. W. Milonni, R. J. Cook, and M. E. Goggin, Phys. Rev. A **38**, 1621 (1988).
[27] A. Sihvola, I. V. Lindell, H. Wallén, and P. Ylä-Oijala, Appl. Comput. Electromagn. Soc. J. **25**, 1007 (2010).
[28] T. H. Boyer, Phys. Rev. A **9**, 2078 (1974).
[29] V. Hushwater, Am. J. Phys. **65**, 381 (1997).
[30] B. Kiani and J. Sarabadani, Phys. Rev. A **86**, 022516 (2012).

[31] J. C. Da Silva, A. Matos Neto, H. Q. Placido, M. Revzen, and A. E. Santana, Physica A **292**, 411 (2001).
[32] J. Sarabadani, B. Ojaghi Dogahe, and R. Podgornik, Europhys. Lett. **112**, 41001 (2015).
[33] N. Kinsey, C. DeVault, A. Boltasseva, and V. M. Shalaev, Nat. Rev. Mater. **4**, 742 (2019).
[34] J. Bohn, T. S. Luk, C. Tollerton, S. W. Hutchings, I. Brener, S. Horsley, W. L. Barnes, and E. Hendry, Nat. Commun. **12**, 1017 (2021).
[35] N. Inui, J. Appl. Phys. **111**, 074304 (2012).
[36] T. Tsutaoka, T. Kasagi, and K. Hatakeyama, J. Appl. Phys. **110**, 053909 (2011).